RESEARCH PAPER

Analyzing the Effect of Mixed Solvent Ratios on the Performance of P3HT: ICxA-Based Organic Solar Cells

Raghad Sabbar Hadi[1,2,*], Furqan Almyahi[1]

* raghad.s.hadi@atu.edu.iq

[1] Department of Physics, College of Science, University of Basrah, Iraq

[2] Department of Laser and Optoelectronics Technical Engineering, Technical Engineering College\Najaf, Al Furat Al Awsat Technical University (ATU), Najaf, Iraq

Abstract: *In this investigation, a formulation was developed as a solution and thin films by combining poly (3-hexylthiophene) (P3HT) and fullerene Indene-C60 multi-adducts (ICxA) with varying solvent ratios. The formulations were prepared under ambient conditions. Morphological parameters were assessed utilizing a transmission electron microscope and scanning electron microscope and complemented by optical microscope pictures. UV-visible absorbance and photoluminescence (PL) measurements were implemented to investigate the optical properties of active layers. The values of the energy gaps of the prepared thin films and solutions increased as the solvent ratios of chlorobenzene to stander solvent increased due to the isolation of P3HT chains from their neighbours. The Raman spectra are associated with high aggregation of composition and increased conformation when the intensity ratio (IC= C/IC-C) is small and the full width at high maximum (FWHM) is low. In ambient conditions, organic photovoltaic cells (OPVs) are produced with varying solvent ratios. The device with a 30% ratio exhibited the highest performance, with a power conversion efficiency (PCE) of approximately 1%, an open circuit voltage (VOC) of 0.571 V, a short circuit current density (JSC) of 7.47 mA.cm^{-2}, and a fill factor (FF) of 38.6%.*

Keywords: Organic solar cells, Chloroform, Chlorobenzene, UV-VIS absorption, Raman spectrum, I-V Characteristics.

1. INTRODUCTION

Organic solar cells convert light energy into electrical energy using organic materials, such as polymers and small organic compounds, instead of inorganic materials, such as silicon, like traditional solar cells [1]. Organic solar cells have essential features that have made them a subject of interest to researchers in renewable energy, such as manufacturing flexibility, flexibility, low cost, diversity of applications, and environmental sustainability, as organic solar cells are considered clean and renewable energy sources. Improving the efficiency and performance of the organic solar cell contributes to reducing our dependence on fossil fuels and reducing carbon emissions, which contributes to achieving environmental sustainability for the future of our planet [2-4]. Solar cells have a composite structure consisting of two main layers: the donor and acceptor layers. These two organic materials participate in converting light energy into electrical charges. When the donor absorbs light, an exciton generation occurs (a pair of electrons and a hole), after which the exciton is stimulated and separated into an electron and a hole [5].

The active layer, a crucial component in the energy conversion process of organic solar cells, is the subsequent destination for the electron onto the electrodes for current generation [6, 7]. P3HT, an acronym for poly(3hexylthiophene), is a light-absorbing donor material that cells utilize. An abundance of electrons that can be transferred to the materials that take light is a defining feature of P3HT. Its low production costs and well-known production procedure make it an excellent material for making solar cells. When exposed to sunlight, Indene-C60 multi-adducts ICxA, an acceptor material, accept electrons from P3HT, which is utilized in solar cells. The exceptional electron-accepting capabilities of this material are well-known to improve solar cell efficiency via carrier transfer [8, 9].

Achieving optimal performance requires simultaneous tuning of the material's band gap energies, HOMO/LUMO levels, and carrier mobilities. We can enhance the performance of materials by annealing them or utilizing solvents when we make them. When it comes to organic solar cells, the active layer development is

affected by the solvent's purity and how quickly it breaks down into components [10]. Solvents with varying melting points and evaporation rates must be mixed to attain stability [11, 12]. This research explores the effect of mixed solvent ratios on the efficiency of P3HT: ICxA-based organic solar cells. By analyzing these cells' optical and electrical properties, we seek to understand the mechanisms that govern the energy conversion process in these devices.

The results of this research have the potential to significantly contribute to the development of new strategies to improve the efficiency of organic solar cells and reduce their cost, bringing us closer to achieving the goal of sustainability in the energy field.

2. EXPERIMENTAL PROCEDURES

2.1. Materials

The polymer Poly(3-hexyl thiophene)(P3HT) with a molecular weight of 20 KDa and the compound ICxA were synthesized in our laboratory using the procedures described in the literature [9]. The ICxA used in this particular batch consists of 36% ICMA, 36% ICMA, 51% ICBA, and 13% ICTA [13-15].They were used as the active layer and poly (ethylene dioxythiophene): poly (styrene sulfonate) (PEDOT: PSS) Clvios as the HTL layer and Zno as an ETL layer ITO-glass(The thickness is roughly 100 nm and the surface resistance ranges from 8 to 12 Ω) substrates as an anode electrode and pure aluminum evaporation wire as cathode electrode, chloroform and chlorobenzene as organic solvents. Almost all materials, tools, and solvents were of high purity and purchased from Ossila Company.

2.2. Preparing Samples

The blend was meticulously prepared by combining P3HT and ICxA with a ratio of 1:1 to get a concentration of 40 mg/mL by dissolution in 1 mL of many solvent ratios (Chloroform (CF) and minor quantities of Chlorobenzene (CB)). The experimental procedure involved adding varying amounts of CB to the primary solvent, namely 0%, 10%, 20%, and 30% for CF. The materials (P3HT: ICxA) were wholly dissolved in solvents through the process of stirring the solutions for two hours at a temperature range of (50-60)°C on a hotplate [16, 17] see Fig 1.

Fig. 1. shows the P3HT:ICxA solutions with (0%, 10%, 20% and 30%) CB

2.3. Devices Fabrication

The fabrication of OPV involves several steps. First, the ITO substrates are thoroughly cleaned with distilled water, acetone, and ethanol, then dried in an electric oven and purified with UV-O3. Next, a hole transport layer, PEDOT: PSS, is spin-coated onto the substrate at 4000 rpm. Then, the active layer is poured at a speed of 2000 rpm. After that, Zno is poured at 4000 rpm for one minute and annealed at a temperature of 140 with a hot plate device. Finally, the mask is placed, and the aluminum electrode is poured into the evaporator. This process is consistent with the literature [18] (see Fig 2).
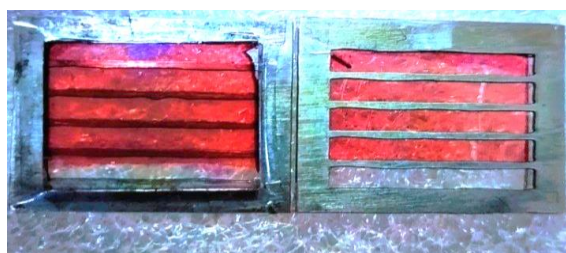

Fig. 2. Image of OSC devices

It is worth noting that the preparation, manufacturing, and measurements were carried out under Non-standard laboratory conditions. The experiment was replicated numerous times, yielding the most favorable outcomes. Following the completion of the bulk preparation method, the upcoming parts will explain the morphology, optical, structure, and electrical features of the active layer of the organic solar cell.

3. RESULTS AND DISCUSSION

3.1. The Morphology Characteristics

3.1.1. *Transmission electron microscopy*

The photographs illustrated the various clusters and forms arising from differing amounts, as depicted in Figure 3, which provides specific details

2

regarding the sample and the solvent's impact.

3.1.2. Scanning electron microscopy

Continuing the previous TEM examinations, we measured the morphology using SEM to provide the necessary information about the sample surface, as shown in Fig. 4.

3.1.3. Optical microscopes

The microscope allows for a comprehensive analysis of the internal composition of materials at the micrometer level, with a magnification factor of 200. An analysis of the collected photos

allows for the evaluation of intricate features about the morphology, repetition, and variations among particles [19]. Optical microscope images provide valuable insights into the intricate details of material morphology and the inherent differences in their internal structures. The images depict the many characteristics of particles, such as color, size, shape, and quantity. These characteristics are influenced by factors such as the type of material, the solvent used, and the preparation technique, mainly when it is done on a large scale. It is shown in Fig 5.

Fig. 3. TEM of a) P3HT:ICxA of 0% CB, b) P3HT:ICxA of 10% CB, c) P3HT:ICxA of 20% CB, d) P3HT:ICxA of 30% CB

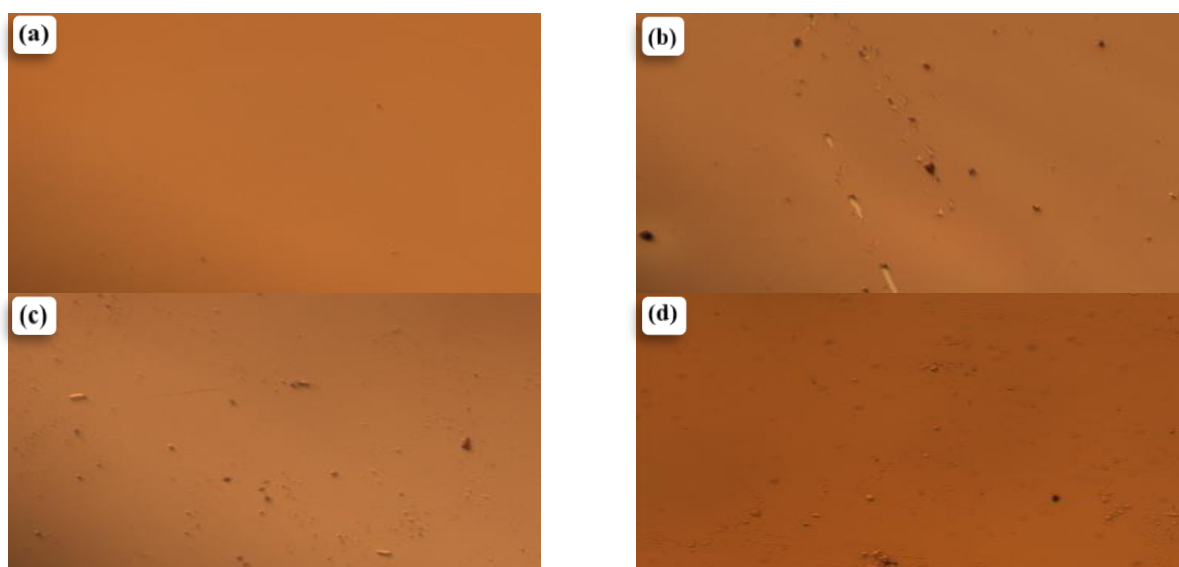**Fig. 4.** SEM of a) P3HT:ICxA of 0% CB, b) P3HT:ICxA of 10% CB, c) P3HT:ICxA of 20% CB, d) P3HT:ICxA of 30% CB

3

Fig. 5. Photomicroscope for a) P3HT, b) ICxA, c) P3HT:ICxA of 0% CB, d) P3HT:ICxA of 10% CB, e) P3HT:ICxA of 20% CB, f) P3HT:ICxA of 30% CB

3.2. Raman Spectra

The molecular structure of BHJ (P3HT: ICxA) dissolved in various solvent ratios was analyzed using Raman spectroscopy technique. Raman spectroscopy can investigate the structure and conformation of polymer backbones. The vibrational frequencies are dictated by the atomic masses and the bond strengths between them. Low Raman shifts are observed when heavy atoms are present and weak bonds are formed. Conversely, high Raman shifts are observed when light atoms are present and strong bonds are formed [20, 10]. The samples were stimulated by a laser that emitted light at a wavelength of 532 nm. A distinct peak in the Raman spectrum (see Fig 6) was observed at wavenumbers (1471, 1477, 1486, 1474) cm^{-1} for the respective ratios (0%, 10%, 20%, 30%), indicating the C=C symmetry stretching of the Thiophen internal vibration ring. In addition, the Thiophen-hexyl internal vibration ring showed peaks at (1401, 1417, 1417, 1411) cm^{-1} for the ratios (0%, 10%, 20%, 30%), which correspond to the vibrations associated with the stretching of the ring. The hexyl molecule in the active layer, at different concentrations (0%, 10%, 20%, 30%), displayed internal vibration characterized by the inter-ring C–C stretch mode at frequencies of 1211, 1211, 1204, and 1198 cm^{-1}, respectively. In addition, another peak was detected due to alkyl vibrations, specifically the stretching of C–C bonds between rings combined with the bending of C–H bonds. This peak's frequencies were measured at (1172, 1158, 1112, 1112) cm^{-1} for the active layers, which have the corresponding compositions of (0%, 10%, 20%, and 30%). The symmetric stretching of C=C bonds and the skeletal stretching of C–C bonds in the thiophene ring, respectively, are responsible for the vibration modes that have been detected. An additional pair of peaks is associated with the C-C stretch mode within the ring and the C-C inter-ring stretch in conjunction with the C-H bending mode. The peak represents the anti-symmetric stretching mode of the C=C bond found at a wavenumber of 1540 cm^{-1} [21].
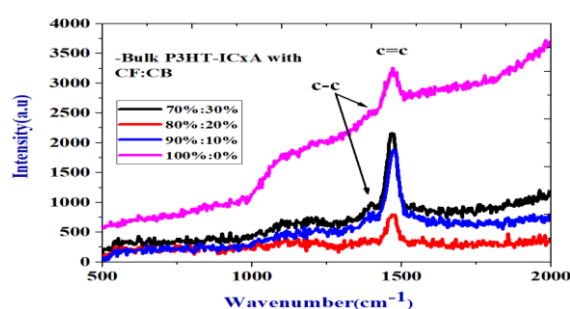

Fig. 6. displays a Raman spectrum for P3HT: ICxA with different solvents ratios

There is no text provided. The Gaussian function fitting technique was employed to examine the peak of symmetric stretching and determine the magnitudes of intensities and the FWHM parameters. The positions of C=C and C-C stretching modes and the relative intensity (IC=C/IC-C) provide valuable information about

4

the films' structural arrangement and molecular structure [22].

Table 1 reveals slight variations in the IC=C/IC-C ratios. This indicates that the ratios do not significantly affect the overall bulk properties. Consequently, the different solvent ratios effectively dissolved and mixed the materials, allowing them to be loaded into the polymer backbone without altering their coupling [23].

3.3. Optical Characteristics

3.3.1. UV-visible spectra

The absorption spectra of P3HT: ICxA generally exhibit broad absorption spectra within the P3HT primary absorption region of 300-650 nm. Typically, peaks in the absorption spectrum signify that the material interacted with light at particular wavelengths, which were defined by the atomic arrangement, material concentration, and experimental conditions. The presence of the primary (maximum) peaks signifies the existence of inter-chain interactions. In contrast, the presence of secondary peaks in the spectrum suggests that the material is highly structured and possesses more mobile and organized chains [18, 24]. The presence of crystalline domains,

interactions between polymer chains, and the conjugation length in the polymer backbone influence the maximum and shoulder peaks. A shorter conjugation length (blue shift) suggests a weaker electronic interaction between the molecules, resulting in increased absorbance. Conversely, a longer conjugation length (redshift) implies a stronger electronic relationship [25] . Consequently, we conducted a comparison of the values in the table and discovered that the primary absorbance and secondary peaks are similar with slight differences caused by the varying quantities of solvents, except for (Fig 7); when examining the solutions, we see distinct absorption peaks without any additional smaller peaks, suggesting that the material has a low reactivity to absorption, the absence of smaller peaks may be due to the material being subjected to annealing at temperatures over 150°, which causes it to exhibit consistent thermal behavior [26]. As for calculating the energy gap for films and solutions, this can be done by using the following [27].

$$Eg= 1240/\lambda \qquad (1)$$

Eg is the energy gap for optical processes and λ is the wavelength of photons.

Table 1. presents the Raman properties

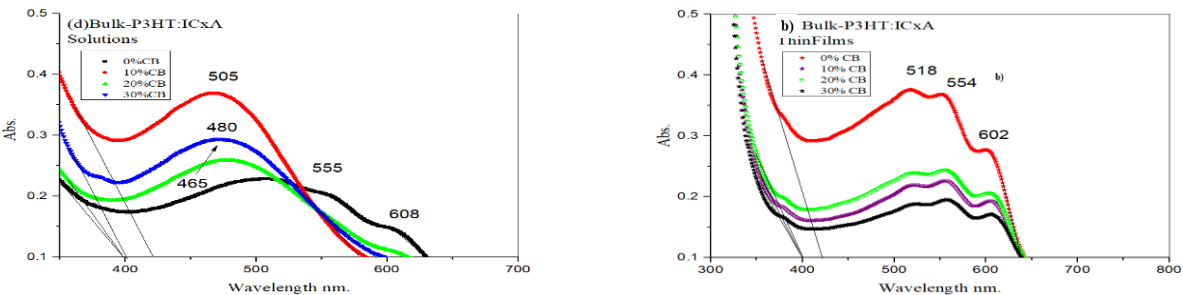| Ratios of (CB%)		Position C=C (cm⁻¹)	Position C-C (cm⁻¹)	Height C=C	Height C-C	$I_{C=C}/I_{C-C}$	FWHM C=C (cm⁻¹)
Bulk	0%	1471	1401	2169.69	995.6	2.17	10.79
	10%	1477	1417	801.25	368.02	1.97	15.027
	20%	1468	1417	1756.85	675.48	2.6	15.027
	30%	1474	1411	1783.9	754.6	2.36	20.47

Fig. 7. depicts the UV-VIS absorption spectra of a) P3HT: ICxA in the form of thin films and b) P3HT: ICxA in the form of solutions

Table 2. shows the Eg (onset) of thin films and solutions

%CB	E.g. (onset) of thin films	E.g. (onset) of solutions
0%	1.9	1.96
10%	1.92	2.141
20%	1.93	2.16
30%	1.937	2.06

3.3.2. The photoluminescence PL spectra

By Fig 8 exhibits the photoluminescence (PL) spectra of Bulk-P3HT: ICxA, which were created using different proportions of CB and stimulated by a 500 nm wavelength of P3HT: ICxA samples, display a wide photoluminescence (PL) emission spectrum with a peak at 588 nm—combining these ratios results in increased solubility, which improves the structure and the likelihood of chain interactions (both within and between transfers).
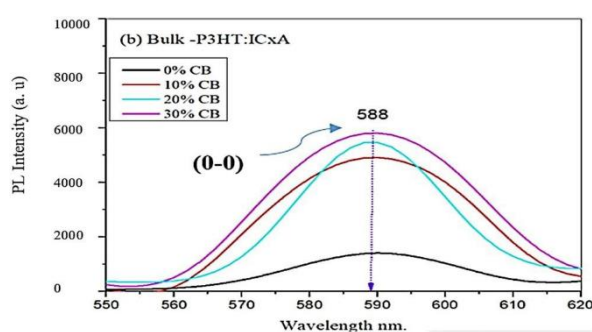

Fig. 8. exhibits the photoluminescence (PL) spectra of Bulk-P3HT: ICxA

A high photoluminescence (PL) intensity is desirable as it indicates a longer lifetime for excitons and enables them to traverse longer distances [28]. In contrast, a diminished photoluminescence (PL) intensity indicates the presence of alternate routes for the rapid dissipation of excitons [29]; these channels accelerate the duration required for an exciton to reach a dissociation site.

3.4. Electricals Characteristics Current Density–Voltage (J-V)

Solar cells having a surface area of 0.06 cm² were evaluated for efficiency utilising various solvent ratios during the mixing procedure. Scientific, a Canadian company, produced the AM1.5 Solar Simulator to take the readings. The simulator gave an intensity of 100 mW/cm². This study examines the current-voltage (J-V) properties of devices made from ITO/PEDOT: PSS/P3HT: ICxA/Zno/Al. The measurements

were undertaken to assess the impact of various solvents on the performance of these devices. According to the examination of the J-V characteristics shown in Fig 9. Photovoltaic performance metrics were collected, such as open circuit voltage (Voc), fill factor (F.F.), series resistance (Rs), shunt resistance (Rsh), and power conversion efficiency (PCE). The summarized values of these parameters are presented in Table 3 for the active layer OPV. The best device performance is achieved with a blend solvent ratio of 30% CB, resulting in a power conversion efficiency (PCE) of (PCE) of 0.998%, a fill factor (F.F) of 38.6, a short circuit current density (Jsc) of 7.472 mA/cm², and an open circuit voltage (Voc) of 0.571 V.

Fig. 9. shows Current density–voltage (J–V) curves for active layer OSC with different (CB) ratios

This combination enhances the surface area to facilitate efficient absorption of light, hence improving the efficiency of the solar cell. To attain a high fill factor (FF), two requirements must be fulfilled: firstly, the shunt resistance must be very high to minimize any leakage currents, and secondly, the series resistance must be meager to guarantee a swift increase in the forward current [30]. Defects and structural deformation in the active layer hinder the movement of charge carriers from the cell to the electrodes.

Table 3. displays the electrical characteristics of the organic solar cells with varying ratios of CB

Active layer	Ratios of CB	V_{oc} (V)	J_{sc} (mA/cm²)	I_{sc} (mA)	F (%)	Series Resistance Ω	Shunt Resistance Ω	PCE (%)
P3HT:ICxA	30%	0.571	7.4722	0. 269	38.6	82.36	4601.88	0.99
	20%	0.566	5.3055	0. 191	39.21	83.08	6647.27	0.71
	10%	0.567	4.305	0. 155	43.04	52.21	9978.1	0.63
	0%	0.590	5.1666	0. 186	30.76	257.5	5055.8	0.56

Additionally, weak junction barriers and reduced shunt resistance can create alternative pathways for the current to flow, decreasing the filling factor. Hence, it is crucial to pay attention to the morphology of the active layer and enhance its homogeneity [31].

4. CONCLUSIONS

This work offers important data on the influence of the solvent ratio in the P3HT: ICxA system, which could be applied in photovoltaic (OSC) systems. Using low ratios of chlorobenzene to the standard solvent (Chloroform), solutions, thin films, and OSCs based on P3HT were investigated. Low-density ratio (IC=C/IC-C) accompanied by diminished full and maximum width (FWHM) in the Raman spectra when the concentration of chlorobenzene in the basic solvent decreases. This pertains to enhanced configuration aggregation and morphology. This was corroborated by transmission electron microscopy, scanning electron microscopy and optical microscopy techniques. The optical absorption spectra exhibited a reduction in intensity with decreasing chlorobenzene ratios, accompanied by a blue shift in the primary peak. Nonetheless, a 10% augmentation in the absorption spectrum's strength relative to other ratios. The emission spectra exhibit an intensification in intensity correlating with the rising proportion of chlorobenzene. Finally photovoltaic cell performance demonstrated an enhancement in PCE with escalating ratios of various solvents. Based on that, it can be concluded that the performance of the CF: CB mixed solvent ratios significantly affect organic solar cells using P3HT: ICxA.

REFERENCES

[1]. Kippelen, B., & Brédas, J. L. "Organic photovoltaics". Energy & Environmental Science, (2009), 2(3), 251-261.

[2]. H. Hoppe and N. S. Sariciftci, "Organic solar cells: An overview," J Mater Res, 2004, vol. 19, no. 7, pp. 1924–1945.

[3]. D. Kearns and M. Calvin, "Photovoltaic effect and photoconductivity in laminated organic systems," J Chem Phys, 1958, vol. 29, no. 4, pp. 950–951.

[4]. K. Petritsch, Organic solar cell architectures. No, 2000.

[5]. Dimitriev, O. P "Dynamics of excitons in conjugated molecules and organic semiconductor systems" Chemical Reviews, 2022, 122(9), 8487-8593.

[6]. M. Marks, Natalie P. Holmes, Anirudh Sharma, Xun Pan, Riku Chowdhury, Matthew G. Barr, Coralie Fenn, Matthew J. Griffith, Krishna Feron, ORCID logo ae A. L. David Kilcoyne, David A. Lewis, Mats R. Andersson, Warwick J. Belchera and Paul C. Dastoor, "Building intermixed donor-acceptor architectures for water-processable organic photovoltaics," Physical Chemistry Chemical Physics, 2019, vol. 21, no. 10, pp. 5705–5715.

[7]. Furqan Almyahi, Thomas R. Andersen, Adam Fahy, Michael Dickinson, Krishna Feron, Warwick J. Belcher and Paul C. Dastoor, "The role of surface energy control in organic photovoltaics based on solar paints," J Mater Chem A Mater, 2019, vol. 7, no. 15, pp. 9202–9214.

[8]. J. Y. Kim, Kwanghee Lee , Nelson E. Coates, Daniel Moses, Thuc-Quyen Nguyen, Mark Dante, and Alan J. Heeger., "Efficient tandem polymer solar cells fabricated by all-solution processing," Science (1979), 2007, Vol. 317, No. 5835, pp. 222–225.

[9]. B. Ali, F. Almyahi, and M. A. Mahdi, "Effect of Poly (3-Hexylthiophene): Mixed Fullerene Indene-C 60 Multi-Adducts Ratios on the Performance of Organic Solar Cells.," Iranian Journal of Materials Science & Engineering , 2023, vol. 20, no. 2.

[10]. Y. S. Kim, Y. Lee, Jai Kyeong Kim, Eun-Ok Seo, Eun-Woo Lee, Wonjoo Lee, Sung-Hwan Han, Soo-Hyoung Lee, "Effect of solvents on the performance and morphology of polymer photovoltaic devices," Current Applied Physics, 2010, Vol. 10, no. 4, pp. 985–989.

[11]. C. V. Kumar, L. Cabau, A. Viterisi, S. Biswas, G. D. Sharma, and E. Palomares, "Solvent annealing control of bulk heterojunction organic solar cells with 6.6% efficiency based on a benzodithiophene donor core and dicyano acceptor units," The Journal of Physical Chemistry C, 2015. vol. 119, no. 36, pp.

20871–20879.

[12]. Y. Chen, C. Zhan, and J. Yao, "Understanding Solvent Manipulation of Morphology in Bulk-Heterojunction Organic Solar Cells," Chemistry–An Asian Journal, 2016, vol. 11, no. 19, pp. 2620–2632.

[13]. K. Landfester R. Montenegro, U. Scherf, R. Güntner, U. Asawapirom, S. Patil, D. Neher, T. Kietzke., "Semiconducting polymer nanospheres in aqueous dispersion prepared by a miniemulsion process," Advanced Materials, 2002, vol. 14, no. 9, pp. 651–655.

[14]. K. Landfester, "Miniemulsion polymerization and the structure of polymer and hybrid nanoparticles," Angewandte Chemie International Edition, 2009, vol. 48, no. 25, pp. 4488–4507.

[15]. Stapleton, Ben Vaughan, Bofei Xue, Elisa Sesa, Kerry Burke, Xiaojing Zhou, Glenn Bryant, Oliver Werzer, Andrew Nelson, A.L. David Kilcoyne, Lars Thomsen, Erica Wanless, Warwick Belcher, Paul Dastoor, "A multilayered approach to polyfluorene water-based organic photovoltaics," Solar energy materials and solar cells, 2012, vol. 102, pp. 114–124.

[16]. H. Tarikhum B, F. Almyahi, and B. Ali, "Optical, Structural, and Electrochemical Properties of P3HT: Y6 Photoactive Layer for Organic Photovoltaics," Karbala International Journal of Modern Science, 2023, vol. 9, no. 4, p. 5.

[17]. F. A. Almyahi, "Optimisation of Aqueous Solar Nanoparticle Inks for Roll to Roll Fabrication of Organic Photovoltaics," The University of Newcastle, 2019 (PhD, 2019).

[18]. K. Yoshida, T. Oku, A. Suzuki, T. Akiyama, and Y. Yamasaki, "Fabrication and characterization of PCBM: P3HT bulk heterojunction solar cells doped with germanium phthalocyanine or germanium phthalocyanine," 2013.

[19]. M. W. Davidson and M. Abramowitz, "Optical microscopy," Encyclopedia of imaging science and technology, 2002, vol. 2, no. 1106–1141, p. 120.

[20]. S. Falke, P. Eravuchira, A. Materny, and C. Lienau, "Raman spectroscopic identification of fullerene inclusions in polymer/fullerene blends," Journal of Raman Spectroscopy, 2011, vol. 42, no. 10, pp. 1897–1900.

[21]. L. G. Bousiakou, H. Gebavi, L. Mikac, S. Karapetis, and M. Ivanda, "Surface enhanced Raman spectroscopy for molecular identification-A review on surface plasmon resonance (SPR) and localised surface plasmon resonance (LSPR) in optical nanobiosensing," Croatica Chemica Acta, 2019, vol. 92, no. 4, pp. 479–494.

[22]. L. Wu ,Santiago Casado, Beatriz Romero, Jose Manuel Otón, Jorge Morgado, Christian Müller, Ruidong Xia, Juan Cabanillas-Gonzalez., "Ground state host–guest interactions upon effective dispersion of regioregular poly (3-hexylthiophene) in poly (9,9-dioctylfluorene-alt-benzothiadiazole)," Macromolecules, 2015 vol. 48, no. 24, pp. 8765–8772.

[23]. B. H. Tarikhum, B. Ali, and F. Almyahi, "Role of Fullerene ICxA and Non-fullerene Y6 in P3HT-based Ternary Organic Photovoltaics," Solid State Commun, 2023, vol. 372, p. 115319.

[24]. M. Manceau, S. Chambon, A. Rivaton, J.-L. Gardette, S. Guillerez, and N. Lemaître, "Effects of long-term UV–visible light irradiation in the absence of oxygen on P3HT and P3HT: PCBM blend," Solar Energy Materials and Solar Cells, 2010, vol. 94, no. 10, pp. 1572–1577.

[25]. K. Petritsch, Organic solar cell architectures. na, 2000.

[26]. U. Bielecka, K. Janus, and W. Bartkowiak, "Nanoaggregation of P3HT in chloroform-anisole solution: relationship between morphology and electrical properties," in Organic Field-Effect Transistors XIII; and Organic Semiconductors in Sensors and Bioelectronics VII, SPIE, 2014, p. 91850E.

[27]. Zhang, Z. G., Liu, H., Wang, X. X., Zhang, J., Yu, M., Ramakrishna, S., & Long, Y. Z. "One-step low temperature hydrothermal synthesis of flexible TiO2/PVDF@ MoS_2 core-shell heterostructured fibers for visible-light-driven photocatalysis and self-cleaning". Nanomaterials, (2019), 9(3), p. 431.

[28]. M. Abdu-Aguye,, Nutifafa Y. Doumon, Ivan Terzic, Jingjin Dong, Giuseppe

Portale, Katja Loos, L. Jan Anton Koster, Maria Antonietta Loi., "Can ferroelectricity improve organic solar cells?," Macromol Rapid Commun, 2020, vol. 41, no. 11, p. 2000124.

[29]. V. Chaudhary, R. K. Pandey, R. Prakash, and A. K. Singh, "Self-assembled H-aggregation induced high performance poly (3-hexylthiophene) Schottky diode," J Appl Phys, 2017, vol. 122, no. 22.

[30]. J. Wang, H. Yao, Y. Xu, L. Ma, and J. Hou, "Recent progress in reducing voltage loss in organic photovoltaic cells," Mater Chem Front, 2021, vol. 5, no. 2, pp. 709–722.

[31]. H. Huang and W. Deng, "Introduction to organic solar cells," in Organic and Hybrid Solar Cells, Springer, 2014, pp. 1–18.